Journal of Applied Polymer Science

Properties and applications of nanoclay reinforced open-porous polymer composites

Elif Yüce,[1] E. Hilal Mert,[1] Sinan Şen,[1] Semih Saygı,[2] Nevim San[2]
[1]Faculty of Engineering, Department of Polymer Engineering, Yalova University, Yalova 77100, Turkey
[2]Department of Chemistry, Yildiz Technical University, Davutpasa Campus, Istanbul 34220, Turkey
Correspondence to: E. H. Mert (E-mail: hmert@yalova.edu.tr)

ABSTRACT: Open-porous nanoclay reinforced polymer composites were prepared via high internal phase emulsion templating using 1,3-butanediol dimethacrylate and surface modified montmorillonite (SM-MMT). Organophilic clay was obtained by using a reactive intercalant—quaternary cocoamine salt having a styryl group—for surface modification of MMT. The clay modification resulted in not only intercalated silicate layers but also nanoclay particles compatible with the continuous phase of the emulsions. It was found that increasing clay amount leads to formation of hierarchical porous structure accompanied with larger cavities and interconnected pores. In this respect, cavity size of the resulting composites was found to be altered between 6.78 and 8.82 μm. On the other hand, as compared to bare composites, addition of clay particles increased compressive modulus of the resulting materials from 26.4 to 72.5 MPa. The adsorption capacities of the porous composites for methyl violet 2B were investigated by batch experiments and discussed as a function of their SM-MMT loading. It was determined that, the dye adsorption of the composites increased with increasing nanoclay amount in the polymer matrix. Thus, the adsorption percentage of the composite loaded with 7 wt % nanoclay was found to be as high as 88%. © 2017 Wiley Periodicals, Inc. J. Appl. Polym. Sci. **2017**, *134*, 45522.

KEYWORDS: adsorption; clay; mechanical properties; morphology; porous materials

Received 6 January 2017; accepted 9 July 2017
DOI: 10.1002/app.45522

INTRODUCTION

High internal phase emulsion (HIPE) templated polymers (polyHIPEs) are known to have an advantage for easy preparation of monoliths,[1,2] beads,[3,4] and membranes,[5,6] exhibiting well-defined hierarchical open-porous structures. HIPEs are concentrated emulsions where higher than 74 vol % of the emulsion contains the internal phase.[7,8] In most cases, deionized water is used as the internal phase while continuous phase consists of monomers. The polymerization of the continuous phase results in highly porous and interconnected crosslinked polymeric foams—polyHIPEs.[9] Depending on their hierarchical porosity, easy control of pore sizes, permeability, and low density, polyHIPEs offer advantages in many fields especially in adsorption,[1,4,10–12] ion exchange,[13,14] chromatography,[15,16] catalysis,[17,18] and tissue engineering.[19–21] However, their insufficient mechanical properties such as brittleness and chalkiness originated from porous morphology prevent their use in major industrial applications.[22,23]

PolyHIPEs were first prepared and patented by the Unilever researchers, Barby and Haq in 1985 from water-in-oil (w/o) HIPEs of styrene (St) and divinylbenzene (DVB).[8] Then, scientists applied several approaches to enhance mechanical properties of polyHIPEs such as by using different monomers that give flexibility and durability to the structure, increasing the crosslinking ratio, adding a suitable reinforcer to continuous phase and increasing the density of material.[22–26] In this respect, silica nanoparticles,[22,23] titania nanoparticles, and carbon nanotubes[27,28] have been used to reinforce different polyHIPE matrices. Among them, montmorillonite and bentonite clays have been mostly used reinforcers for the preparation of high strength polyHIPE foams. For instance, Pakeyangkoon *et al.* prepared polyDVB polyHIPEs filled with porous clay particles by using organomodified bentonite and reported that presence of layered silicate in the polymer matrix resulted in improved compressive stress and Young's modulus of the material up to 84% and 137%, respectively.[29] Abbasian and Moghbeli reported polyHIPE nanocomposites from HIPEs having styrene/acrylonitrile/organoclay and revealed that adding 3 wt % of hydrophilic organoclay to the polymer matrix improved crush strength significantly.[30] Recently, Alikhani and Moghbeli reported polyHIPE nanocomposite foams from the polymerization of organically modified montmorillonite containing vinylbenzyl chloride/divinylbenzene (VBC/DVB) HIPEs.[13] In this study, they showed

that presence of 1 wt % nanoclay enhances both Young's modulus and crush strength of the resulting materials. More recently, Çira *et al.* prepared polyHIPE/clay composites by using a reactive intercalant and achieved to improve thermal and mechanical properties of the materials.[26]

Although many scientists have investigated the influence of several reinforces, particularly nanoclay particles on the polyHIPE morphology and mechanical properties, researchers have not been focused on the morphological properties, mechanical strength, and thermal stability at the same time. Moreover, most of the studies subjecting the use of nanoclay particles were based on brittle polyHIPE structures which were usually obtained by the polymerization of styrene and/or DVB.[13,26,29,30]

In current study, in order to prepare high mechanical strength and adsorptive polyHIPEs for organic dyes, methacrylate based polyHIPE/clay composites were synthesized from 1,3-butanediol dimethacrylate (1,3-BDDMA) and a reactive surface modified montmorillonite (SM-MMT) containing HIPEs. The resulting polyHIPE composites, to the best of our knowledge, which were obtained without using a rigid comonomer, were not reported in the polyHIPE literature by this time. With this approach, thanks to the synergistic contribution of the flexible monomer and reactive nanoclay, polyHIPEs exhibiting relatively high mechanical strength were obtained without compromising pore structure.

In order to obtain organophilic clay, a quaternary salt of cocoamine having a styryl group was used as a reactive intercalant for surface modification of MMT. Apart from the previous studies, the reactive styryl group of the SM-MMT clay was believed to take part in the polymerization/crosslinking reaction of HIPEs which may cause formation of an exfoliated polyHIPE composite with enhanced mechanical strength. Subsequent work explored the use of these materials as adsorbents for organic dyes. Accordingly, adsorptive properties of resulting materials were characterized by batch experiments. With this respect, methyl violet 2B (MV) was chosen for the adsorption experiments as a result of this dye is frequently detected in wastewaters of various industries such as textile, cosmetics, paper, and so forth due to its application in dyeing. It is well known that organic dyes including MV are carcinogenic and cause hypersensitivity reactions in humans.[31–33] The removal of MV from water was studied for the bare polymer foam and the resulting composites prepared with different nanoclay loadings (1, 3, and 7 wt % of SM-MMT). We show that polyHIPE/clay composites, which were obtained by the polymerization of 1,3-BDDMA in w/o type HIPEs with the presence of SM-MMT, are good candidates as adsorbent materials for the removal of organic dyes.

EXPERIMENTAL

Materials

1,3-BDDMA (99%, contains 150–250 ppm MEHQ as an inhibitor) and PluronicL-121 which is a poly(ethylene glycol)-*block*-poly(propylene glycol)-*block*-poly(ethylene glycol) copolymer ($M_n \sim 4400$) were purchased from Sigma-Aldrich (St. Lois, USA) and used without further purification. 2,2′-Azobissobutyronitril (AIBN) was commercial grade and used after recrystallization from ethanol.

The sodium montmorillonite clay (NaMMT) was kindly donated by Süd Chemie, (Moosburg, Germany) (Nanofil 1080; cationic (Na^+) exchange capacity of 100 mequiv/100 g). The synthesis and characterization of quaternary cocoamine salt was reported in a previous study of Helvacioglu *et al.*[34] The chemical structure of quaternary cocoamine salt, having a vinyl group and a tail with up to 18 carbons composed of about 6% C8, about 4% C10, about 48% C12, about 21% C14, about 11% C16, and about 10% C18 alkyl chains.[34] The modification of NaMMT with cocoamine salt was reported previously by Tekay and Şen.[35]

MV (indicator grade, dye content: 75%) was supplied from Sigma-Aldrich Company and used as received. Ethanol was technical grade and in all experiments ultrapure deionized water was used.

Preparation of PolyHIPE/Clay Composites

The continuous phase of the HIPEs were prepared by mixing 1,3-BDDMA, emulsifier (Pluronic L121), nanoclay particles, and polymerization initiator (AIBN) in a reaction vessel. In order to determine the influence of preparation conditions on the physical properties of the resulting materials, emulsifier amount was changed between 20 and 30 vol % (regarding to continuous phase), while the internal phase ratio was altered between 75 and 95 vol % (regarding to total emulsion volume). Moreover, the effect of the amount of nanoclay loading was determined by changing the nanoclay loading between 1, 3, or 7 wt % (regarding to continuous phase). In a typical experiment in which HIPEs have 75 vol % of nominal porosity and 30 vol % of surfactant, polyHIPE/clay composites were prepared by mixing 1,3-BDDMA (6.4375 g, 28.46 mmol), 1, 3, or 7 wt % of SM-MMT (regarding to continuous phase), Pluronic L121 (1.5719 g, 0.35 mmol), and AIBN (0.0467 g, 0.28 mmol, 1 mol % regarding to 1,3-BDDMA) in a 250 mL two-necked round bottom flask. Once a homogeneous mixture was obtained, deionized water (18.75 mL) was added dropwise with constant stirring at 300 rpm. After the addition of the internal phase was completed, the mixture was stirred for further 30 min. Then, the obtained emulsion was transferred to a polyethylene mold and cured at 70 °C for 24 h. Afterward, the resulting polyHIPE/clay composites were purified via Soxhlet extraction (ethanol, for 24 h) and dried in a vacuum oven at 50 °C. The bare polyHIPE foam was also prepared according to procedure the described above without adding SM-MMT.

Characterization

Structural Analyses. X-ray diffraction (XRD) measurements were conducted using a Rigaku D/Max-Ultimate diffractometer (Rigaku, Tokyo, Japan) with Cu Kα radiation ($\lambda = 1.54$ Å), operating at 40 kV and 40 mA and a scanning rate of 0.2 deg/min.

Morphological Properties. Pore morphology of the resulting polyHIPEs was investigated by scanning electron microscopy (SEM) using ESEM-FEG and EDAX Philips XL-30 microscope (Philips, Eindhoven, the Netherlands). Average cavity diameters were calculated by taking at least 50 measurements from each

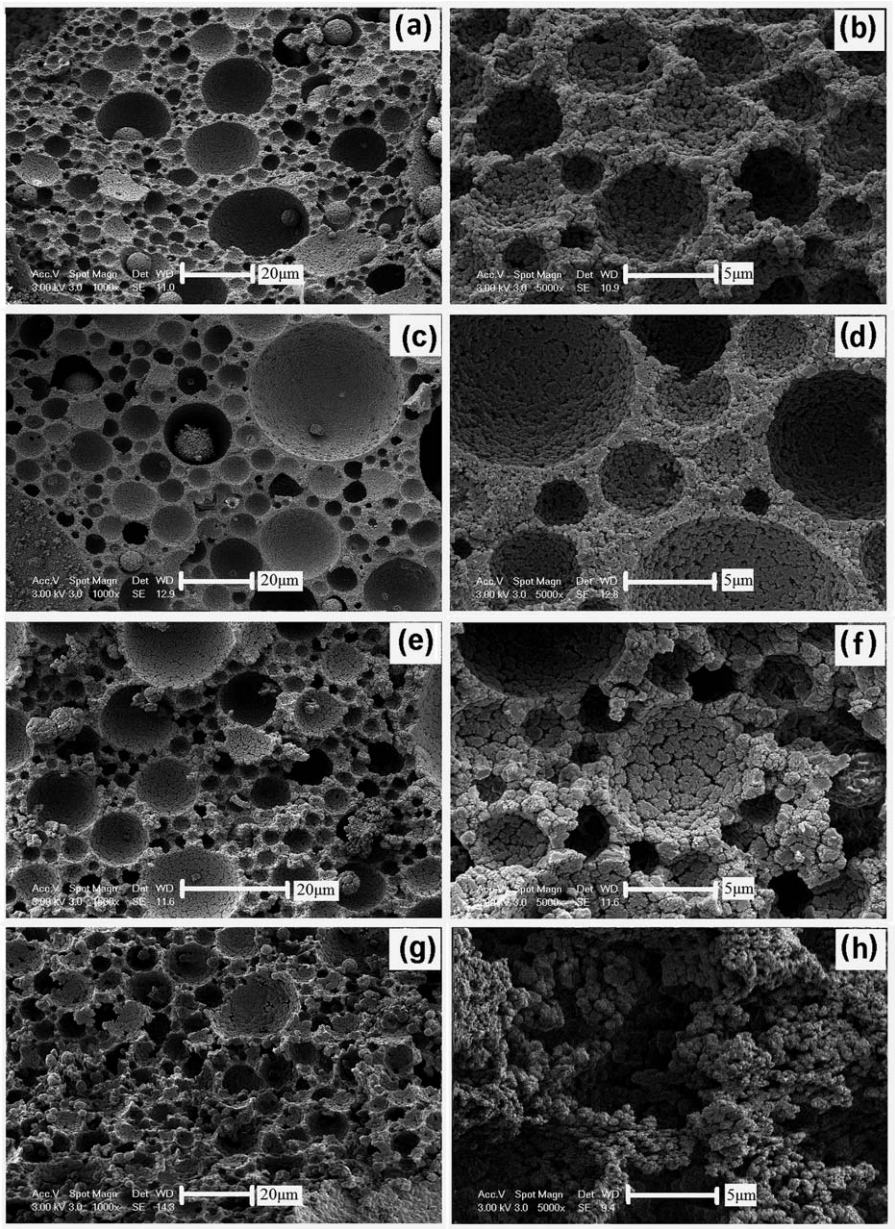

Figure 1. SEM images of polyHIPEs obtained by using different surfactant amounts during HIPE preparation: (a,b) 15 vol %, (c,d) 20 vol %, (e,f) 25 vol %, and (g,h) 30 vol %.

SEM image and the average value was corrected with a correction factor ($2/3^{1/2}$) to account for irregular cutting of the samples.[36]

Surface areas and average pore diameters were measured with Micromeritics Gemini VII Surface Area and Porosity Analyzer (Micromeritics Instrument Corporation, USA) by applying the Brunauer–Emmet–Teller (BET) equation on N_2 adsorption/desorption isotherms. Prior to analysis, all samples were degassed for 24 h at room temperature in Micromeritics FlowPrep 060 Sample Degas System (Micromeritics Instrument Corporation, USA).

Mechanical Properties. Compressive properties of the polyHIPEs were measured with a Zwick/Roell Z020 Universal Testing Machine (Zwick GmbH & Co.KG, Germany) equipped with a 20 kN load cell according to ASTM D1621–2004 standard by applying uniaxial compression load. For each sample, the measurements were repeated for three specimens at a compression rate of 1.3 mm/min. Compressive strength and compression modulus were calculated as the average value of three different measurements.

Thermal Stability. Thermogravimetric analysis (TGA) of the polyHIPEs was performed on a Seiko TG/DTA 6300 thermal analysis system instrument (Seiko Instruments Inc., Tokyo, Japan) under nitrogen flow with a heating rate of 10 °C/min.

Batch Adsorption Experiments. Adsorption studies were conducted by using bare polyHIPE monolith and polyHIPE

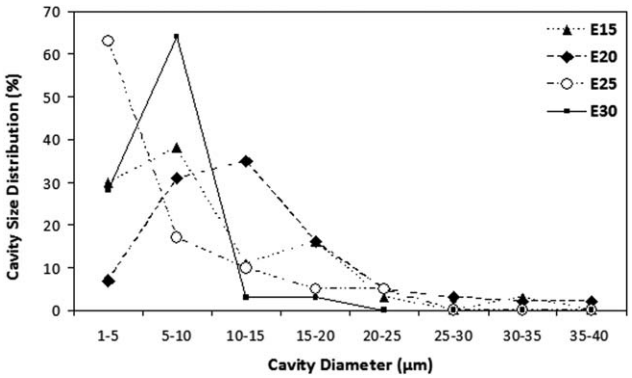

Figure 2. Distribution of cavities for polyHIPEs obtained from the HIPEs stabilized by using 15 vol % (E15), 20 vol % (E20), 25 vol % (E25), and 30 vol % (E30) of emulsifier.

composites reinforced with 1, 3, or 7 wt % of SM-MMT in a batch system. In the experiments, an aqueous solution of a cationic dye, MV, was used. With this respect, stock solution containing 200 mg L^{-1} of MV was prepared and the required concentrations of the dye were taken from this solution by dilution. All adsorption studies were executed at natural pH (5.1) of the dye solutions. In a typical experiment, batch adsorption study was accomplished by adding 0.1 g polyHIPE material and 25 mL of diluted MV solution containing 10 mg L^{-1} into a 100 mL Erlenmeyer flask. Then, the mixture was agitated in a horizontal shaking water bath at a constant speed and temperature (150 rpm, 25 °C). After 5 h, the polyHIPE material was removed from the solution and the remaining solution was filtered to ensure that all free adsorbent particles were removed. Then, the concentration of the remaining MV in the solution was determined by using a single beam UV–visible spectrophotometer (Shimadzu UV-vis Mini 1240) at the maximum wavelength (λ_{max}) of 584 nm. The concentration of MV was determined by using a linear calibration curve and percentage of the removed dye was calculated according to eq. (1), where C_0 is the initial concentration of MV (mg L^{-1}) and C_t is the concentration of MV at any time t.

$$\text{Adsorption } (\%) = \frac{(C_0 - C_t)}{C_0} \times 100 \quad (1)$$

RESULTS AND DISCUSSION

The water-in-oil (w/o) HIPEs of 1,3-BDDMA was prepared by using Pluronic L121, which is a block copolymer of ethylene oxide and propylene oxide. It is a commercial nonionic surfactant containing 10 wt % of hydrophilic ethylene oxide group

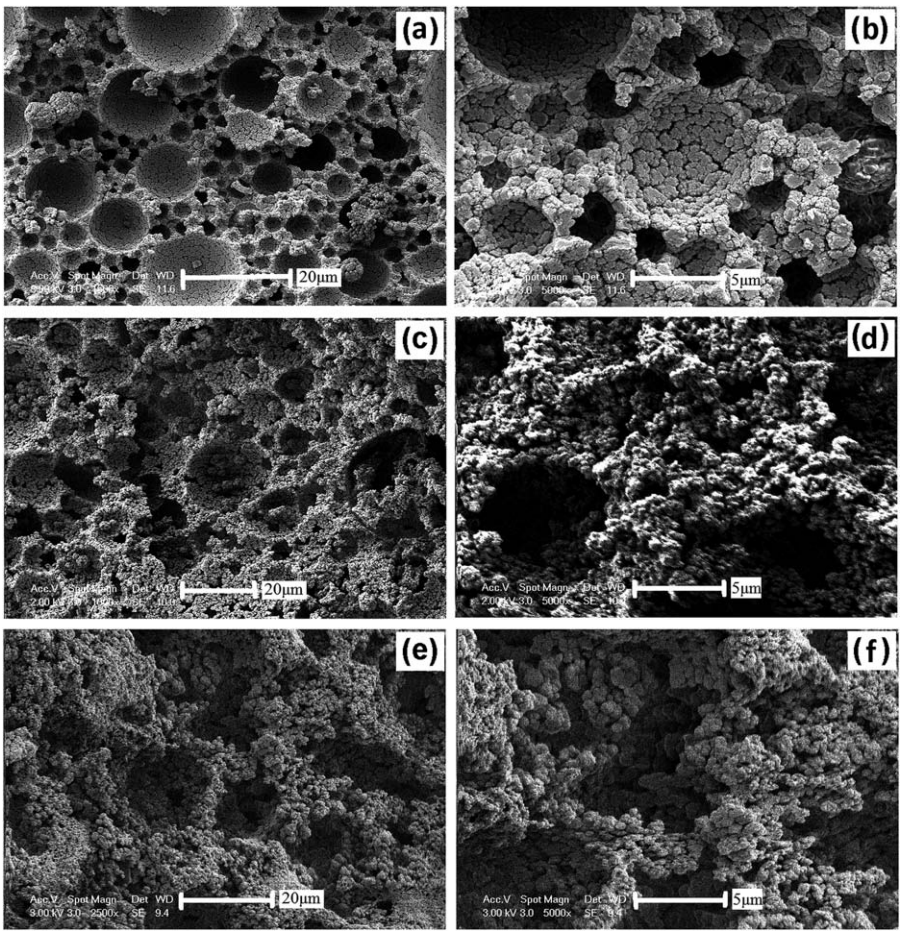

Figure 3. SEM images of polyHIPEs obtained by using different amounts of internal phase in preparation of HIPE: (a,b) 75 vol %, (c,d) 80 vol %, and (e,f) 85 vol %.

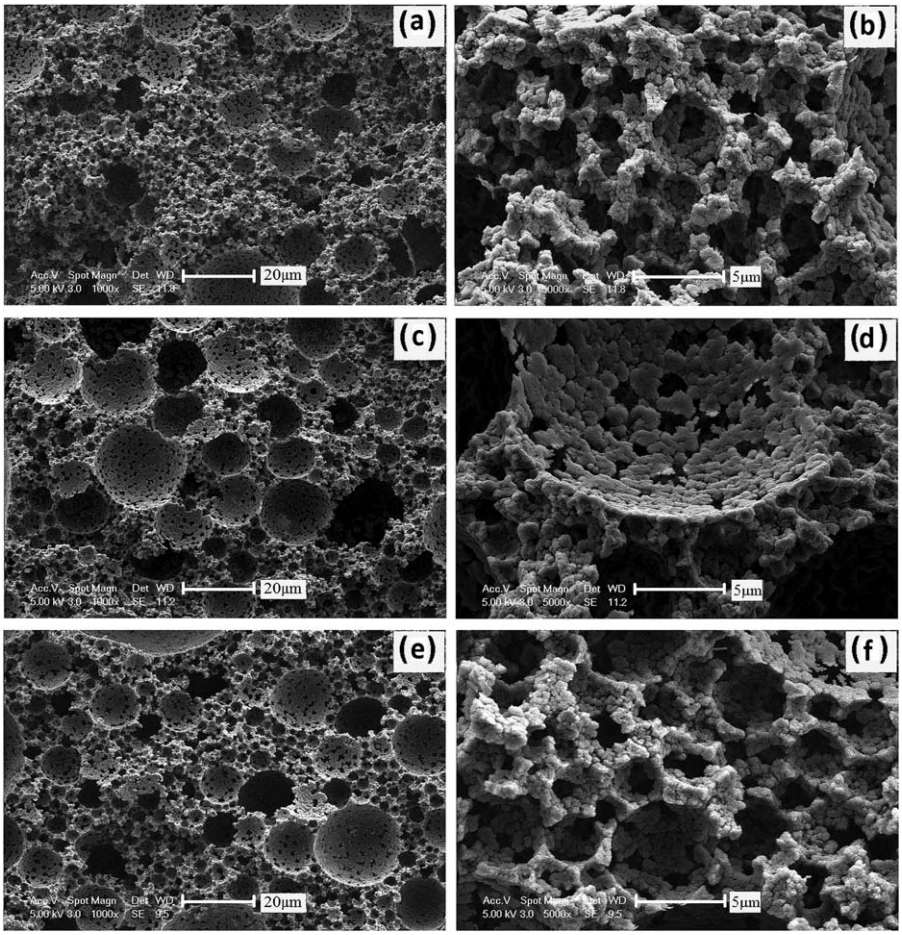

Figure 4. SEM images of polyHIPE composites obtained by loading different amounts of nanovaly: (a,b) 1 wt %, (c,d) 3 wt %, and (e,f) 7 wt %.

and has a hydrophile–lipophile balance (HLB) which is close to 1.0. In order to prepare a stable water-in-1,3-BDDMA HIPE, the surfactant amount was varied between 15 and 30 vol %. The influence of surfactant amount on polyHIPE morphology was investigated by SEM analyses which are given in Figure 1. According to given SEM images, lower surfactant amounts (15 and 20 vol %) were found to be insufficient for stabilizing emulsions. The signs of phase inversion can be clearly observed from Figure 1(a–d). Bead like polymer particles located in the cavities are thought to form as a result of phase inversion. The formed bead like particles can be explained by the monomer molecules diffused to the internal phase (deionized water). The secondary particles seen in the cavity structures are most probably due to polymerization of the diffused monomers there.[37]

In addition, from the cavity size calculations done according to SEM images, average cavity sizes of the polyHIPEs obtained from the HIPEs prepared by 15 and 20 vol % emulsifier (samples E15 and E20, respectively) were found to be 7.96 and 12.89 μm, respectively. Moreover, both materials exhibits hierarchical cavity size distribution according to the SEM based cavity size calculations (Figure 2). Increasing surfactant amount to 25 vol % resulted in desired morphology consisting of an open-porous and hierarchical cavity size distribution [Figure 1(e,f)]. SEM images given in Figure 1(e,f) also revealed that using 25 vol % of surfactant in preparation of emulsion increased the emulsion stability by preventing phase inversion and bead formation. Moreover, it was also observed from Figure 1 that the cavity size distribution became narrower with increase in amount of

Table I. Results of the SEM Characterization and BET Surface Area Measurements of Bare PolyHIPE Foam and PolyHIPE Composites

PolyHIPE	SM-MMT (wt %)	Cavity size (μm)	Interconnected pore diameter (μm)	S_{BET} (m^2 g^{-1})
E25	—	7.45 ± 0.17	—	18.1
PH-1	1	6.78 ± 0.05	1.18 ± 0.01	20.2
PH-3	3	8.82 ± 0.18	1.42 ± 0.01	18.2
PH-7	7	8.77 ± 0.21	1.44 ± 0.01	16.5

Table II. XRD Data for Clays and PolyHIPE Composites

Material	d_{001} of clay (Å)[a]
NaMMT[32]	12.13 (7.28°)
SM-MMT[32]	25.81 (3.41°)
PH-1	—
PH-3	39.83 (2.16°)
PH-7	49.85 (1.77°)

[a] Two-theta angles are given in parentheses.

the surfactant. This result can be attributed to the reduction in droplet coalescence.[38] On the other hand, at a higher surfactant amount (30 vol %), the walls have lost some of their structural integrity. Accordingly, the continuous polymeric framework that was observed in the polyHIPE sample having 25 vol % of surfactant was disturbed. In this case, some sign of wall break up which causes partial collapse of spherical cavities were observed from Figure 1(g,h). These observations seem to be consistent with average cavity diameters calculated from SEM images of the related materials. While the emulsifier amount increased from 25 to 30 vol %, average cavity size of the resulting materials decreased slightly from 7.45 to 6.26 μm, respectively. However, cavity size distributions narrowed with the increased emulsifier amount (Figure 2). In case of polyHIPE obtained from the HIPE having 25 vol % emulsifier (E25), approximately 63% of all cavities were between 1 and 5 μm, 17% of all cavities were between 5 and 10 μm, 10% of all cavities were between 10 and 15 μm, 5% of all cavities were between 15 and 20 μm, and 5% of all cavities were between 20 and 25 μm. On the other hand, cavity size distributions were calculated approximately as 28%, 64%, 3%, and 3% for the cavities that were between 1 and 5 μm, 5 and 10 μm, 10 and 15 μm, and 15 and 20 μm, respectively, for the polyHIPE obtained from the HIPE prepared by 30 vol % emulsifier (E30).

The influence of internal phase on the resulting polyHIPEs was investigated by using different amounts of the internal phase (75–95 vol %). It was observed that higher internal phase ratios caused emulsion destabilization and the HIPEs were phase separated during polymerization at 70 °C. Consequently, emulsions having 90 and 95 vol % of internal phase did not result in robust polyHIPE monoliths. On the other hand, polyHIPE monoliths were obtained from the polymerization of HIPEs prepared by using 75, 80, and 85 vol % of internal phase. The influence of internal phase ratio on the polyHIPE morphology was investigated by SEM analyses (Figure 3). It is seen from Figure 3 that increasing internal phase amount hinders the development of hierarchical cavities. This situation can be explained by the water solubility of 1,3-BDDMA. With the use of monomers having different degrees of water solubility's, the increase in amount of internal phase enhances diffusion of monomers to this phase. Consequently, in addition to phase inversion, droplet coalescence can also be used to expound the observed cell structure in Figure 3(c–f). Based on the given SEM images in Figure 3, it was concluded that a 75 vol % internal phase with respect to total volume of emulsion seems to be an optimum internal phase ratio.

In order to improve the morphological, and mechanical properties of poly(1,3-BDDMA) polyHIPEs, 1, 3, and 7 wt % of SM-MMT nanoclay was introduced into the continuous phase of HIPE templates. The influence of nanoclay amount on the morphological properties of resulting polyHIPE composites was basically determined by using SEM analyses (Figure 4). It is clearly seen from Figure 4 that the amount of nanoclay has a

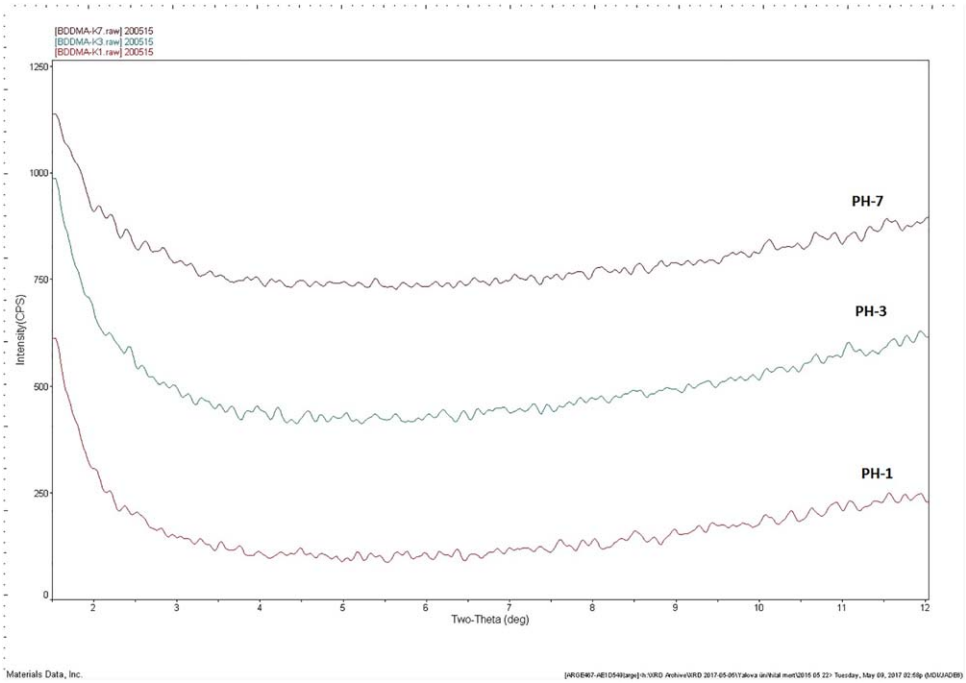

Figure 5. XRD pattern of polyHIPE composites. [Color figure can be viewed at wileyonlinelibrary.com.]

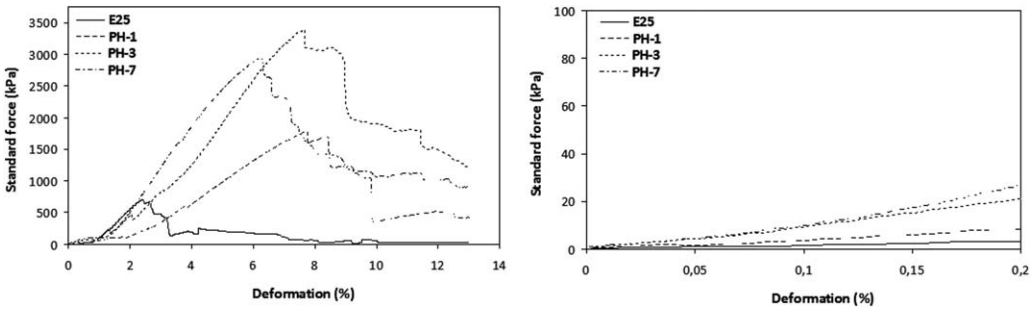

Figure 6. Mechanical characterization of polyHIPEs under compressive force.

significant role on the formation of interconnected pores between large cavities. This result can be attributed to the use of quaternary salt of cocoamine with a styryl moiety as a reactive intercalant for the modification of nanoclay. The reason for uniform dispersion of the aqueous phase droplets in the continuous phase can be most probably due to the presence of the intercalant on the clay enhancing emulsion stability.[38] As a result, it was concluded that increasing nanoclay amount increases the pore interconnectivity and improves morphological properties of the resulting composites.

Average cavity diameters and interconnected pore diameters calculated by using SEM images of the relating materials are presented in Table I. According to SEM based calculations, the average cavity diameter of the bare poly(1,3-BDDMA) was found to be 7.45 μm, while it was 6.78, 8.82, and 8.77 μm for the polyHIPE composites having 1, 3, and 7 wt % of nanoclay, respectively (Table I). This result shows that, as compared to bare poly(1,3-BDDMA), addition of 1 wt % nanoclay slightly decreases average cavity diameter of the resulting polyHIPE composite. On the other hand, with the increase in nanoclay amount average cavity diameter also increases slightly. In addition, the interconnected pore diameters were found to be significantly influenced by the presence of nanoclay particles in the polymer matrix. As well as the cavities in the bare polyHIPE [Figure 2(a,b)] were connected by cracks on the cavity walls, resulting in nanocomposites with spheroidal interconnected pores (Figure 4). This result can be accepted as an indication of enhanced emulsion stability and uniform dispersion of the aqueous phase droplets in the continuous phase via help of SM-MMT clay particles. SEM based calculations of interconnected pore diameters for polyHIPE composites (Table I) demonstrate that the amount of nanoclay has a slight influence on the size of pores. The interconnected pore diameters were found to be 1.18, 1.42, and 1.44 μm for the composites having 1, 3, and 7 wt % of nanoclay, respectively (Table I). In addition to SEM investigation, the influence of nanoclay amount was also determined by measuring surface area of resulting materials. Surface areas were calculated by applying the BET equation to the N_2 adsorption/desorption isotherms and given in Table I. According to the given data, as compared with the bare poly(1,3-BDDMA) polyHIPE, the surface area (S_{BET}) of the resulting composites was first increased slightly with the addition of 1 wt % nanoclay, and then decreased again slightly. The S_{BET} of the bare poly(1,3-BDDMA) was found to be 18.1 m^2 g^{-1} while it was measured as 20.2 and 16.5 m^2 g^{-1} for the composites having 1 and 7 wt % of nanoclay, respectively.

The intercalation of the surface modification agent (quaternary cocoamine salt) in between silicate layers of SM-MMT clay was previously confirmed by XRD analyses (Table II) in the study of Tekay and Şen.[35] Herein, XRD analysis was also used for the structural characterization of the resultant polyHIPE composites. The results of XRD characterization are given in Figure 5 and Table II. It is seen from the XRD diffractograms that, polyHIPE composite having 1 wt % of nanoclay has no noticeable clay peak appearing in the XRD patterns. This result can be attributed to the homogeneous dispersion of clay layers in the poly(1,3-BDDMA) matrix, which demonstrates that polyHIPE composite reinforced with 1 wt % of SM-MMT revealed an exfoliated nanocomposite structure.[30,35] On the other hand, increasing nanoclay amount resulted in a lower diffraction angle and higher *d*-spacings the polyHIPE composites having 3 and 7 wt % of nanoclay. In these cases, (001) diffraction peaks existed

Table III. Mechanical and Thermal Properties of Bare PolyHIPE Foam and PolyHIPE Composites

PolyHIPE	SM-MMT (wt %)	E_c [a] (MPa)	σ_c [b] (MPa)	T_{d10} (°C)	T_{d50} (°C)	V_{max} (wt % min^{-1})	T_{max} (°C)	Char (wt %)
E25	—	26.4	0.09	254.4	309.2	10.67	312.9	0.5
PH-1	1	35.8	0.10	255.4	307.2	10.89	309.7	1.1
PH-3	3	57.9	0.08	257.2	303.1	11.66	306.1	2.1
PH-7	7	72.5	0.09	247.2	295.1	10.05	294.3	2.6

[a] E_c: compression modulus.
[b] σ_c: compressive strength.

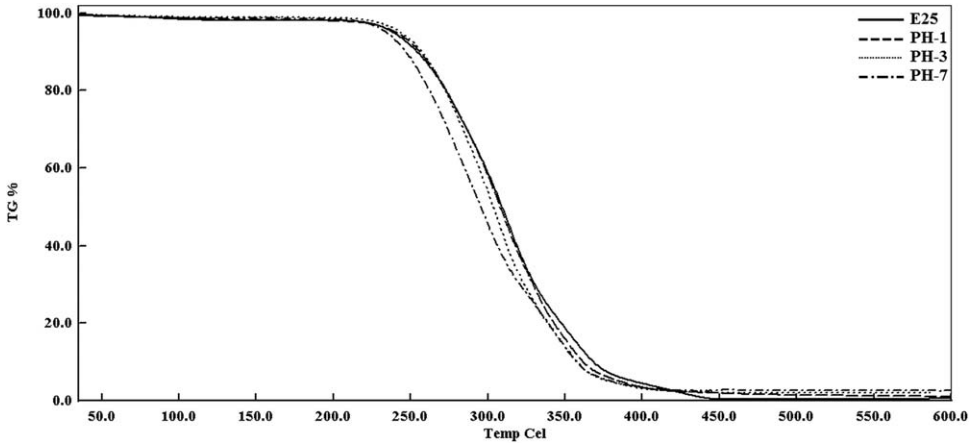

Figure 7. The thermogravimetry (TG) curves of the polyHIPEs.

at 2.16° and 1.77° were related to *d*-spacings 39.83 and 49.85 Å. This increment of interlayer spacing can be accepted as an indication for a partially intercalated structure.[35,39]

PolyHIPEs are known to be very fragile and brittle materials due to their highly porous interconnected structure.[7,9] In this respect, with use of a relatively flexible monomer and SM-MMT nanoclay, more durable polyHIPE composites as compared to analogues polyHIPE materials were obtained as reported in the literature.[24,26,29,30] Mechanical properties of resultant polyHIPEs were investigated in terms of compression modulus and compressive strength and the results are presented in Figure 6 and Table III. The results showed that the presence of SM-MMT nanoclay has a great influence on the mechanical strength of polyHIPEs. Moreover, it was also found that with the increasing amount of nanoclay, compression modulus of the resulting composites was improved significantly. As compared to bare poly(1,3-BDDMA), addition of 1, 3, and 7 wt % nanoclay into the polyHIPE matrix caused almost 1.4, 2.2, and 2.7 times higher compression moduli for the related composite samples (Table III). The increment in the compression moduli of the polyHIPE composites may also be attributed to the reactive double bonds in the intercalant by participating in the polymerization reaction which present additional crosslinks to the system and so increasing the mechanical strength. Thus, the surface modification group covalently connects to the polymer skeleton.[35] On the other hand, participation of clay particles in the polymerization may cause higher amount of ionic interactions between positively charged quaternary ammonium groups of the ammonium salt and the negatively charged clay surfaces which are bonded to the main crosslinked networks. Consequently, in addition to chemical bonding of the SM-MMT clay to the polymer matrix, the interaction between the counter charged parts may lead to a stretchable microcomplex structure.[26] These types of reversible physical interactions are known to cause a viscous character that helps materials to share the applied compression forces more effectively. Accordingly, the strength and compressibility of the resulting materials are increased.[40–42] But in our case, compression test was performed according to ASTM D1621–2004 standard and for all materials the test was automatically ended by the software at 13% of elongation was reached. Thus, at relatively higher strength of 1 wt % clay loading, composite can be ascribed to well dispersion of clay particles which may result in an optimized amount of reversible ionic crosslinks in the matrix. On the other hand, while maintaining high strength much higher moduli values at

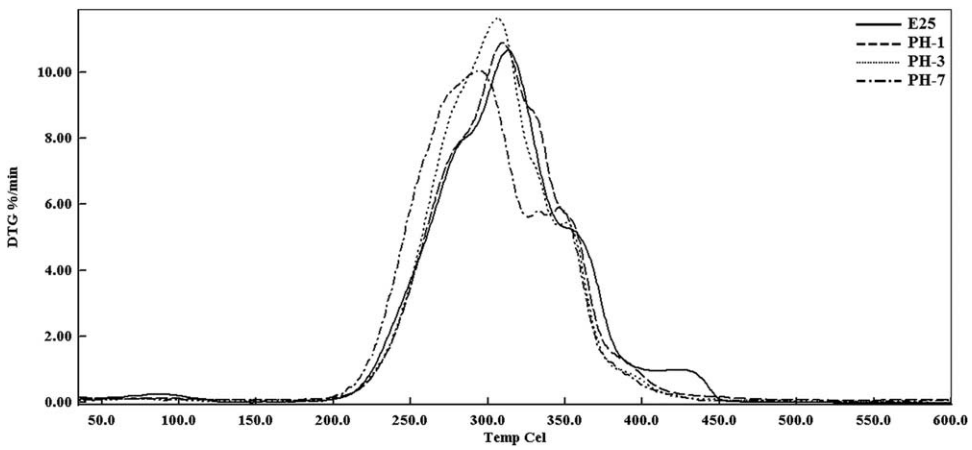

Figure 8. The derivative thermogravimetry (DTG) curves of the polyHIPEs.

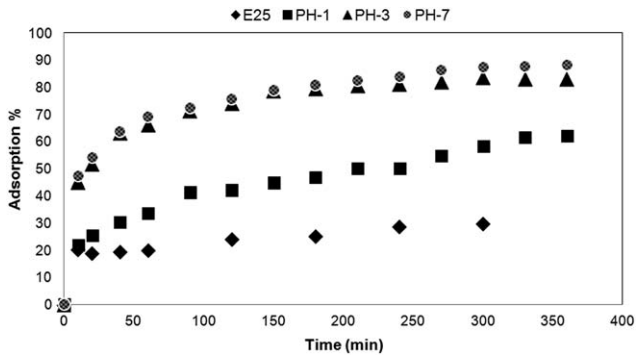

Figure 9. Dye adsorption capacities of polyHIPEs.

higher clay loadings can also be due the same physical interactions together with the chemical crosslinking contribution of the clay.

Thermal stabilities of bare polyHIPE and polyHIPE/SM-MMT composites were investigated by TGA. The comparative thermogravimetry and derivative thermogravimetry (TG and DTG) curves are presented in Figures 7 and 8. In addition, the decomposition temperatures at 10% and 50% weight loss (T_{d10} and T_{d50}), the maximum decomposition rate (V_{max}), the maximum decomposition temperature (T_{max}) and residual char at 600 °C are summarized in Table III. According to TG curves given in Figure 7 that both resulting composites and bare polyHIPE exhibited two stage continuous weight loss up to about 430 °C. The massive weight loss for all materials was started at around 225 °C and continued to almost 370 °C. At the end of continuous weight loss the residual char was calculated as 0.5, 1.1, 2.1, and 2.6 wt % for the bare polyHIPE and the composites having 1, 3, and 7 wt % of nanoclay, respectively. In addition, the onset and the midpoint decomposition temperatures (T_{d10} and T_{d50}) were estimated from the DTG thermograms given in Figure 8. It was found that the change of T_{d10} for the composites having 1 and 3 wt % of nanoclay was negligible as compared to bare polyHIPE sample. However, it was decreased 7 °C for the composite prepared by loading 7 wt % of nanoclay. It was also observed as compared to bare polyHIPE that T_{d50} and T_{max} temperatures of the composites were decreased significantly with the increasing nanoclay amount. Moreover, as compared to bare polyHIPE variation of V_{max} with nanoclay loading was also found to be insignificant.

Figure 10. The image of (a) polyHIPE composite reinforced by 1 wt % of nanoclay and (b) the dye solution before and after adsorption experiment. [Color figure can be viewed at wileyonlinelibrary.com]

Herein, we also demonstrate that the obtained polyHIPEs can be effectively used for the adsorption of an organic dye. In this respect, we studied the adsorption of a cationic dye, MV, from water. MV is a hazardous dye, which has an extensive application in textile industry.[43] The dye uptake capacities of the bare polyHIPE and polyHIPE composites having 1, 3, and 7 wt % SM-MMT were investigated by conducting batch experiments and the comparative dye uptake capacities of the resulting materials are presented in Figure 9. Moreover, the image of the polyHIPE adsorbent having 1 wt % of nanoclay and the dye solution before and after adsorption experiment is also presented in Figure 10. It was determined by the batch experiments that the bare polyHIPE sample exhibited the lowest adsorption capacity for MV dye, as expected. On the other hand, introduction of nanoclay particles into the polymer matrix caused a significant increment on dye adsorption. This result may be attributed to the participation of clay particles in the polymerization reaction which may cause higher amount of interactions between positively charged quaternary ammonium groups of the surface modifier salt and the negatively charged clay surfaces. Accordingly, the increase in the amount of nanoclay also resulted in higher adsorption capacities for the resultant composites. The adsorption capacities were found to be 31%, 66%, 83%, and 88% for the bare polyHIPE and the composites reinforced by 1, 3, and 7 wt % of nanoclay, respectively.

CONCLUSIONS

In this article, novel polyHIPE materials with relatively high mechanical strengths were prepared by the polymerization of w/o type HIPEs. With this respect, a flexible methacrylate monomer having a butanediol group was used to create a stretchable polymer matrix. Moreover, the polymer matrix was reinforced by introducing nanoclay particles into the continuous phase of the HIPEs during emulsification. In order to prevent emulsion destabilization in the presence of nanoparticles, quaternary cocoamine salt modified MMT (SM-MMT) was used as reinforcing agent. Thanks to the chemical structure of the surface modifier group, the stabilization of water droplets in the oil phase was enhanced by quaternary cocoamine salt. In addition, the styryl end group contributed to the crosslinking reaction. The influence of nanoclay addition into the polymer matrix was investigated in terms of morphological and mechanical properties. It was found that loading of 1, 3, and 7 wt % SM-MMT significantly increases mechanical strength of the resulting composites, while it enhances formation of interconnected and

open-porous cavities as compared to bare polyHIPE matrix. Moreover, by using XRD, exfoliation and intercalation of clays in polymer matrix were confirmed. Dye adsorption behavior of the composites was investigated via batch adsorption tests. In the tests, removal of a cationic dye—MV—from water was studied for the composites with different nanoclay loadings (1, 3, and 7 wt % of SM-MMT). It exhibited that increasing amount of nanoclay in the polymer matrix caused higher dye adsorption for the composites. In addition, the adsorption percentages of the composites loaded with 1, 3, and 7 wt % nanoclay were found to be 66%, 83%, and 88%, respectively which are much higher than that of bare polyHIPE polymer (31%) as a beneficial effect of the clay used.

REFERENCES

1. Mert, E. H.; Kaya, M. A.; Yıldırım, H. *Des. Monomers Polym.* **2012**, *15*, 113.
2. Jerenec, S.; Šimic, M.; Savnik, A.; Podgornik, A.; Kolar, M.; Turnšek, M.; Krajnc, P. *React. Func. Polym.* **2014**, *78*, 32.
3. Desforges, A.; Arponteta, M.; Deleuze, H.; Mondain-Monval, O. *React. Func. Polym.* **2002**, *53*, 183.
4. Mert, E. H.; Yıldırım, H. *e-Polymers* **2014**, *14*, 65.
5. Kovaćić, S.; Preishuber-Pflügl, F.; Slugovc, C. *Macromol. Mater. Eng.* **2014**, *299*, 843.
6. Sevšek, U.; Seifried, S.; Stropnik, Č.; Pulko, I.; Krajnc, P. *Mater. Technol.* **2011**, *45*, 247.
7. Silverstein, M. S. *Polymer* **2014**, *55*, 304.
8. Barby, D.; Haq, Z. U.S. Pat. 4,522,953 (June 11, **1985**).
9. Silverstein, M. S. *Progr. Polym. Sci.* **2014**, *39*, 199.
10. San, N.; Mert, E. H.; Kaya, D.; Çira, F. *Fresen. Environ. Bull.* **2016**, *25*, 3635.
11. Mert, H. H.; Şen, S. *e-Polymers* **2016**, *16*, 419.
12. Huš, S.; Kolar, M.; Krajnc, P. *J. Chromatogr. A* **2016**, *1437*, 168.
13. Alikhani, M.; Moghbeli, M. R. *Chem. Eng. J.* **2014**, *239*, 93.
14. Hainey, P.; Sherrington, D. C. *React. Funct. Polym.* **2000**, *43*, 195.
15. Tunç, Y.; Gölgelioğlu, Ç.; Hasırcı, N.; Ulubayram, K.; Tuncel, A. *J. Chromatogr. A* **2010**, *1217*, 1654.
16. Zhang, Q.; Yang, G.; Liu, H.; Jing Yang, Y.; Yan, L. B. *J. Chromatogr. Sci.* **2010**, *48*, 517.
17. Çetinkaya, S.; Khosravi, E.; Thompson, R. *J. Mol. Catal. Chem.* **2006**, *254*, 138.
18. Kovačič, S.; Anžlovar, A.; Erjavec, B.; Kapun, G.; Matsko, N. B.; Žigon, M.; Žagar, E.; Pintar, A.; Slugovc, C. *ACS Appl. Mater. Interfaces* **2014**, *6*, 19075.
19. Christenson, E. M.; Soofi, W.; Holm, J. L.; Cameron, N. R.; Mikos, A. G. *Biomacromolecules* **2007**, *8*, 3806.
20. Hayward, A. S.; Eissa, A. M.; Maltman, D. J.; Sano, N.; Przyborski, S. A.; Cameron, N. R. *Biomacromolecules* **2013**, *14*, 4271.
21. Owen, R.; Sherborne, C.; Paterson, T.; Green, N. H.; Reilly, G. C.; Claeyssens, F. *J. Mech. Behav. Biomed. Mater.* **2016**, *54*, 159.
22. Menner, A.; Haibach, K.; Powell, R.; Bismarck, A. *Polymer* **2006**, *47*, 7628.
23. Wu, R.; Menner, A.; Bismarck, A. *J. Polym. Sci., Part A: Polym. Chem.* **2010**, *48*, 1979.
24. Funda, Ç.; Mert, E. H. *Polym. Eng. Sci.* **2015**, *55*, 2636.
25. Mert, E. H.; Slugovc, C.; Krajnc, P. *Express Polym. Lett.* **2015**, *9*, 344.
26. Çira, F.; Berber, E.; Şen, S.; Mert, E. H. *J. Appl. Polym. Sci.* **2015**, *132*, DOI: 10.1002/app.41333.
27. Menner, A.; Salgueiro, M.; Shaffer, M. S. P.; Bismarck, A. *J. Polym. Sci., Part A: Polym. Chem.* **2008**, *46*, 5708.
28. Qian, H.; Greenhalgh, E. S.; Shaffer, M. S. P.; Bismarck, A. *J. Mater. Chem.* **2010**, *20*, 4751.
29. Pakeyangkoon, P.; Magaraphan, R.; Malakul, P.; Nithitanakul, M. *J. Appl. Polym. Sci.* **2009**, *114*, 3041.
30. Abbasian, Z.; Moghbeli, M. R. *J. Appl. Polym. Sci.* **2011**, *119*, 3728.
31. Kooh, M. R. R.; Dahri, M. K.; Lim, L. B. L.; Lim, L. H.; Malik, O. A. *Environ. Earth Sci.* **2016**, *75*, 783.
32. Vargasa, A. G.; Lima, E.; Ortega, G. A. U.; Tolentino, M. A. O.; Rodríguez, E. E. *Appl. Surf. Sci.* **2016**, *363*, 372.
33. Hameed, B. H. *J. Hazard. Mater.* **2008**, *154*, 204.
34. Helvacioglu, E.; Aydın, V.; Nugay, T.; Nugay, N.; Uluocak, B. G.; Şen, S. *J. Polym. Res.* **2011**, *18*, 2341.
35. Tekay, E.; Şen, S. *Int. Polym. Process.* **2015**, *30*, 248.
36. Barbetta, A.; Cameron, N. R. *Macromolecules* **2004**, *37*, 3202.
37. Berber, E.; Çira, F.; Mert, E. H. *Polym. Compos.* **2016**, *37*, 1531.
38. Williams, J. M.; Gray, A. J.; Wilkerson, M. H. *Langmuir* **1990**, *6*, 437.
39. Alexandre, M.; Dubois, P. *Mater. Sci. Eng. R: Rep.* **2000**, *28*, 1.
40. Haraguchi, K.; Takehisa, T.; Fan, S. *Macromolecules* **2002**, *35*, 10162.
41. Haraguchi, K.; Li, H. J. *Macromolecules* **2006**, *39*, 1898.
42. Haraguchi, K.; Farnworth, R.; Ohbayashi, A.; Takehisa, T. *Macromolecules* **2003**, *36*, 5732.
43. Kooh, M. R. R.; Lim, L. B. L.; Lim, L. H.; Bandara, J. M. R. S. *Waste Biomass Valorization* **2015**, *6*, 547.